1   Glycerol configurations of environmental GDGTs investigated using a selective *sn*2 ether

2   cleavage protocol

3

4   Xiao-Lei Liu [a]*, David A. Russell [b], Claudia Bonfio [b], Roger E. Summons [c]

5

6   [a] Department of Geology and Geophysics, University of Oklahoma, Norman, OK 73019,

7   USA

8   [b] MRC Laboratory of Molecular Biology, Francis Crick Avenue, Cambridge CB2 0QH,

9   UK

10   [c] Department of Earth, Atmospheric, and Planetary Sciences, Massachusetts Institute of

11   Technology, 77 Massachusetts Avenue, Cambridge, MA 02139-4307, USA

12

13   * Corresponding author, Xiao-Lei Liu

14

15

16   E-mail address: xlliu@ou.edu

17

18

19   **Abstract**

20   The glycerol configurations of glycerol dialkyl glycerol tetraethers (GDGTs) in

21   environmental samples were investigated using a selective *sn*2 ether cleavage protocol.

22   Using this procedure, GDGTs with a parallel glycerol configuration afford two types of

23   derivatives, diols and diallylethers, whereas only one kind, monoallylethers, originate

24   from their antiparallel isomers. Isoprenoidal GDGTs from a marine sediment are shown

25   to be predominately parallel based on the distributions of these ether cleavage products.

26   Crenarchaeol and its so-called regioisomer both have parallel configurations with the

27   cyclohexane ring located on the *sn*3,3 ether bonded tricyclic biphytanyl moiety. A Messel

28   shale sample containing isoprenoidal GDGTs contributed mainly by methanogenic

29   archaea has a substantial portion with the antiparallel configuration. Branched (non-

30   isoprenoidal) GDGTs in both the Messel shale and the marine sediment are mainly

31   antiparallel. This selective *sn*2 ether cleavage approach provides a potentially powerful

32   analytical tool to investigate not only the exact molecular structures of GDGT

33   constitutional isomers and their biosynthetic pathways but also to evaluate the

34   heterogeneous inputs of sedimentary GDGT and their isotopic signatures, if different

35   source species synthesize GDGTs with unique glycerol configurations. Further analyses

36   of this type will reveal the glycerol configurations of the GDGTs of a broad range of

37   microbial cultures and environmental samples.

38   **Key words:** GDGT, chemical degradation, glycerol configuration, crenarchaeol, marine

39   sediment, methanogen

40

1. INTRODUCTION

Isoprenoidal GDGTs are distinctive bipolar membrane-spanning lipids exclusively synthesized by Archaea. The intact polar lipids of archaeal tetraethers comprise, in general, three molecular components, namely the polar head groups, the isoprenoidal hydrocarbon chains and the glycerol backbones (Fig. 1). Structural diversity of archaeal tetraethers is recognized in the variety of polar head groups; modifications - including hydroxylation, cyclization, unsaturation and methylation - to the isoprenoidal hydrocarbon chains; and the two types of glycerol arrangements, the parallel and antiparallel configurations (Fig. 1). The widely applied analytical method of liquid chromatography-mass spectrometry (LC–MS) combined with various ionization approaches, such as atmospheric pressure chemical ionization (APCI), electrospray ionization (ESI) and matrix-assisted laser desorption/ionization (MALDI), can readily distinguish GDGTs with different polar headgroups and hydrocarbon chains, but is not capable of distinguishing between the parallel and antiparallel glycerol constitutional isomers.

Gräther and Arigoni (1995) designed a chemical degradation sequence of reactions to cleave ether bonds specifically at the *sn*2 glycerol carbon, so that the glycerol configurations of precursor GDGT could be deduced from the composition of the degradation products. By conducting this selective *sn*2 ether cleavage reactions on the acyclic isoprenoidal GDGT (GDGT-0) isolated from three archaeal cultures, *Methanobacterium thermoautotrophicum, Thermoplasma acidophilum* and *Sulfolobus solfataricus,* Gräther and Arigoni (1995) reported an approximately 1:1 ratio of the parallel and antiparallel GDGT-0 regioisomers further speculating that the biosynthesis of archaeal tetraethers involved no preference for either type of glycerol configuration.

65   However, our recent investigation on the ***natural degradation*** derivatives of

66   environmental archaeal tetraethers indicated a predominantly parallel glycerol

67   configuration in marine sediments and substantial antiparallel configuration in sediments

68   that were strongly influenced by methanogenic activity (Liu et al., 2018). To further

69   verify our detection of GDGT glycerol configurations in natural depositions, we adapted

70   the ***chemical degradation*** protocol of Gräther and Arigoni (1995) to investigate the

71   glycerol configurations of environmental GDGTs.

72

73   **2. EXPERIMENTAL**

74   **2.1. Sample collection and preparation**

75   A commercial mixture of glyco-GDGT-phosphoglycerol (gly-GDGT-PG), the

76   main phospholipids of *Thermoplasma acidophilum*, was purchased from Matreya LLC

77   (PA 16803, USA), and used as a representative sample to verify and improve the

78   chemical degradation protocol reported by Gräther and Arigoni (1995). Around 1 μg of

79   this intact polar GDGT mixture was first hydrolyzed with 10% HCl in methanol at 70 °C

80   for two hours to yield the core GDGTs. Two environmental samples, a marine sediment

81   from ODP201 1227A and the Messel shale (excavation site E 8/9, horizon 2.5–3.5 m),

82   were dried and powdered and approximately 2 g of each sample was extracted following

83   the modified Bligh and Dyer protocol described previously (Sturt et al., 2004) to yield

84   total lipid extracts (TLEs).

85   **2.2. Selective *sn*2 ether cleavage**

86   An aliquot of each sample was transferred into a 2 mL glass vial and dried with a

87   stream of nitrogen (N_2) for chemical degradation. We adapted the first sequence of

88   reactions described by Gräther and Arigoni (1995) for our investigation (reaction scheme

89   shown in Fig. 2). Briefly, core GDGTs were first tosylated with an excess amount (10

90   mg) of *p*-toluenesulfonyl chloride (Sigma-Aldrich) in 100 µL pyridine (Sigma-Aldrich) at

91   room temperature for three days. Then, 500 µL of 5 N aqueous HCl and 500 µL *n*-hexane

92   were added to the reaction vial and the two phases were mixed vigorously by vortexing.

93   After separation of the two phases, the organic phase, containing tosylated GDGTs, was

94   transferred into another 2 mL vial. The aqueous phase was extracted a further three times

95   with *n*-hexane and the organic extracts were combined and dried under a stream of N_2 for

96   further reaction. To cleave the *sn*2 ether bonds, 10 mg of sodium iodide (NaI, Sigma-

97   Aldrich) and 10 mg of zinc powder (purum grade, Sigma-Aldrich) were added to the

98   residue from the previous reaction and the mixture was suspended in 100 µL 1,2-

99   dimethoxyethane (DME, Sigma-Aldrich) and heated at 90 °C for two hours. Degradation

100 products were finally retrieved by liquid-liquid extraction using 500 µL of water and 500

101 µL *n*-hexane and then vortexing. The two phases were separated, and, as before, the

102 aqueous phase was extracted a further three times with *n*-hexane. Finally, the combined

103 organic phases were dried in a 2 mL vial for analysis.

104 **2.3. Lipid analysis with LC–MS**

105   Lipid analysis by LC–MS was performed on an Agilent 1290 series UPLC system

106 coupled to an Agilent 6530 qTOF mass spectrometer through an Agilent jet stream dual

107 electrospray ionization (AJS–ESI) interface. The ESI drying gas (N_2) temperature was set

108 at 300°C, the N_2 flow rate was 8 L min^{-1} and the nebulizer gas (N_2) pressure was 35 psi.

109 The qTOF parameters were set to: capillary voltage 3.5 kV, fragmentor voltage 175 V;

110 skimmer voltage 65 V and octopole voltage 750 V in auto MS/MS scanning mode with

111 MS^1 range of *m/z* 100-3000 and MS^2 mass range of *m/z* 50-3000.

112   Separation of compounds was achieved with a reverse phase LC method modified

113   from Zhu et al. (2013). Briefly, samples were dissolved in methanol and injected with a

114   volume of 10 μL onto an Agilent Zorbax Eclipse XDB-C18 column (1.8 μm, 4.6 × 100

115   mm; Agilent) maintained at 35 °C. Mobile phase flowed at a rate of 0.5 mL min^{-1}, first

116   isocratically with 100% A for 2 min, followed by a gradient to 40% B at 15 min, and to

117   90% B at 40 min, and then to 100% B at 41 min and hold for 14 min, and finally re-

118   equilibrated with 100% A for 10 min, where the eluent A was 100:0.04:0.10 of

119   methanol/formic acid/14.8 M NH$_3$(aq.) and B was 100:0.04:0.10 of 2-propanol/formic

120   acid/14.8 M NH$_3$(aq.).

121

122   **3. RESULTS**

123   **3.1. Lipid composition of samples prior to their chemical degradation**

124   Core GDGTs released by acid hydrolysis from the gly-GDGTs-PG of *T.*

125   *acidophilum* consist of GDGT-0 to GDGT-6 (Fig. 3A1). The TLE of marine sediment,

126   ODP201_1227A, is dominated by GDGT-0 and crenarchaeol (cren-a) with a small

127   proportion of GDGT-1 to -3, hydroxyl GDGTs (OH-GDGTs) and branched GDGTs. The

128   putative crenarchaeol regioisomer (cren-b) elutes prior to cren-a under reverse phase

129   condition. Substantial amounts of biphytanediols (bpdiols), which consist of mainly

130   bpdiol-0 and -cren, occur as natural degradation product of GDGTs (Fig. 3B1 and

131   Supplementary Fig. S1). The Messel shale extract exhibits a GDGT distribution that is

132   typical of sulfidic lacustrine settings (Liu et al., 2016) in which branched GDGTs are

133   relatively more abundant than isoprenoidal GDGTs and GDGT-0 is the major

134   isoprenoidal GDGT and accompanied by S-GDGTs as minor components (Fig. 3C1).

3.2. Detection of degradation derivatives

135

136   The major ionized forms of GDGTs and their corresponding degradation

137   derivatives, the bpdiol and the monoallyl biphytanol monoether (mbpm), are their

138   protonated molecular ions, $[M+H]^+$. However, the other type of degradation product, the

139   diallyl biphytanyl diether (dbpd), is detected mainly in the form of its ammonium adducts,

140    $[M+NH_4]^+$. All three categories of degradation derivatives, bpdiol, dbpd and mbpm,

141   occur in the sample of *T. acidophilum* after ether cleavage, but each group has a different

142   ring distribution (Fig. 3A2 and Supplementary Fig. S2). Three bpdiols with up to two

143   rings are released by ether cleavage. A later eluting peak (labeled as '?') following the

144   monocyclic bpdiol (bpdiol-1) occurs and partially co-elutes with bpdiol-2. The MS^2

145   fragmentation pattern of this compound is very different from those of bpdiols (Fig. S4),

146   and it could not be identified as a bpdiol isomer. The monoallylether derivatives are the

147   most abundant degradation products and consist of mbpm-0 to -3 (Supplementary Fig.

148   S2). Dbpds contain however up to 4 rings. When subjected to chemical degradation

149   isoprenoidal GDGTs in the Messel shale also produce all three types of degradation

150   derivatives (Fig. 3C2 and Supplementary Fig. S3). So far no clear signal of S-GDGT

151   related degradation derivatives can be distinguished for those of regular GDGTs.

152   Degradation derivatives in both *T. acidophilum* and Messel shale exhibit a mbpm-

153   dominated distribution pattern. However, GDGTs in the marine sediment,

154   ODP201_1227A, produce almost exclusively bpdiol and dbpd as their degradation

155   products except for the trace amount of mbpm-0 (Fig. 3B2). Acyclic and tricyclic

156   derivatives (dbpd-0 and -cren-a) prevail over other dbpds in the chemically degraded

157   marine sediment (Supplementary Fig. S1). Bpdiols contain up-to two rings with no

158   tricyclic derivatives detected (Supplementary Fig. S1).

159   Given the high abundance of branched GDGTs in the Messel shale extracts, all

160   three types of degradation products (diols, monoallylethers and diallylethers) are detected

161   (Fig. 4A). Degradation derivatives of branched (non-isoprenoidal) GDGT in

162   ODP201_1227A are less abundant compared to those in Messel shale sample (Fig. 4B).

163   Monoallylethers prevail over diols and diallylethers in both samples, and the

164   monoallylethers in Messel shale and marine sediment are dominated by dimethyl and

165   trimethyl derivatives, respectively (Fig. 4).

166

167   **4. DISCUSSION**

168   **4.1. Reactions of selective *sn*2 ether cleavage**

169   In the process of chemical degradation the two free hydroxyl groups of core

170   GDGTs are first tosylated with *p*-toluenesulfonyl chloride in pyridine at room

171   temperature for three days. The tosylated GDGTs are then heated with sodium iodide and

172   zinc powder in DME at 90 ºC for 2 hours. The tosylates are converted into the

173   corresponding iodides *in situ* (Fig. 2) and the iodides undergo zinc-mediated Boord

174   haloalkoxy elimination (Dykstra *et al.* 1930). In this way, the *sn*2 ether bonds are cleaved

175   and double bonds were formed affording an allyl substituent in the remaining ether (Fig.

176   2). As shown in Fig. 2, cleavage of the *sn*2 ether bonds on a GDGT with parallel glycerol

177   configuration gives two degradation products, the bpdiol that was originally ether-bonded

178   to the glycerol *sn*2 carbons and the remaining dbpd. However, *sn*2 ether cleavage on an

179   antiparallel GDGT results in two mbpms.

180   The ratio of mbpm/(bpdiol+dbpd) of chemically degraded *T. acidophilum* is

181   approximately 1:1, which indicates a mixture of parallel and antiparallel configured

182   precursor GDGTs in nearly equal abundance. Such a result is consistent with the previous

183   report on *T. acidophilum* by Gräther and Arigoni (1995) and validates this selective *sn*2

184   ether cleavage protocol.

4.2. Antiparallel GDGT of methanogenic input

186   The thermophilic methanogen, *M. thermoautotrophicum*, has been known to

187   produce both parallel and antiparallel GDGTs in ~1:1 ratio (Gräther and Arigoni, 1995).

188   Archaeal lipids preserved in the Messel shale are primarily derived from methanogenic

189   archaeal communities (Hayes et al., 1987; Bauersachs et al., 2014). The approximately

190   1:1 ratio of mbpm/(bpdiol+dbpd) in chemically degraded Messel shale extracts suggests

191   that mesophilic methanogens synthesize GDGTs similar to those of their thermophilic

192   relatives, with both parallel and antiparallel configurations. Our previous analysis on

193   natural degradation derivatives in seep carbonate (Liu et al., 2018) also points to the idea

194   that environments rich in contributions from Euryarchaeota, including methanogens, will

195   be dominated by antiparallel GDGTs..

4.3. Predominant parallel glycerol configuration of marine archaeal GDGTs

197   The remarkable abundances of bpdiol and dbpd with a minor mbpm-0 as the

198   degradation derivatives of ODP201_1227A show that the precursor GDGTs in marine

199   sediment possess a predominantly parallel configuration (Fig. 3B2). The predominance of

200   bpdiol and dbpd chemical degradation products confirms unambiguously what we have

201   observed with the distribution of natural degradation derivatives in various marine

202   subsurface sediments (Liu et al., 2018). Since isoprenoidal GDGTs in our previously

203   analyzed marine sediments (cf. Table 1 of Liu et al., 2018), especially those from open-

204   ocean slope settings, are primarily derived from planktonic species, mainly marine

205   *Thaumarchaeota* (Pearson et al., 2016), we can hypothesize that marine *Thaumarchaeota*

206 predominantly synthesize parallel glycerol configured GDGTs. The minor mbpm-0

207 represents a small proportion of antiparallel GDGT-0 either synthesized by

208 *Thaumarchaeota* or contributed by other archaeal taxa. We also noticed in our previous

209 investigation that the natural degradation product of antiparallel GDGT, *sn*2,3-GMGD

210 (glycerol monobiphytanyl glycerol diether), is either absent or present in very low

211 abundance in most sediments collected from regular marine deposits, but has been

212 observed in substantial amounts in one particular sample affected by anaerobic methane

213 oxidation (AOM) (Liu et al., 2018).

214 **4.4. The structures of crenarchaeol and its isomer**

215 Conventional, non site-specific, ether cleavage can only show that there is one

216 tricyclic biphytane originating from cren-a and a further two different tricyclic isomers

217 with distinct ring configurations originating from cren-b (Liu et al., 2018; Sinninghe

218 Damsté et al., 2018). However, our studies of degradation products from both natural

219 diagenesis and chemical degradation reveal not only the distinct ring configurations but

220 also the glycerol configuration and the location of the cyclohexyl ring. Bpdiol-cren-a and

221 -b exist in the TLE of marine sediment as natural degradation products (Fig. 3B1), but

222 there is no tricyclic bpdiol generated through the selective *sn*2 ether cleavage. The

223 occurrence of dbpd-cren-a and -b with equally abundant bpdiol-2 confirms our previous

224 deductions concerning the molecular structures of cren-a and -b. Degradation products of

225 cren-a and -b released from either natural diagenesis or selective *sn*2 ether cleavage

226 indicate that both are parallel in glycerol configuration, but with different *sn*3,3 ether-

227 bonded tricyclic biphytanes (see crenarchaeol structure illustrated in Fig. 3B1). Further

228 studies are still required to determine the precise ring structures in cren-a and -b.

229 **4.5. Glycerol configuration of branched GDGTs**

230   All three classes of degradation products, diols, monoallylethers and diallylethers,

231   were detected after chemical degradation of branched GDGTs in Messel shale extracts

232   and in the ODP201_1227A extract. Their co-occurrence suggests the existence of both

233   parallel and antiparallel glycerol configured branched GDGTs in our analyzed samples.

234   The much higher abundance of monoallylether relative to diols and diallylether suggests

235   that branched GDGTs are mainly antiparallel in the glycerol configuration (Fig. 4) in

236   these two types of depositions, marine and sulfidic lakes. It is shown that branched

237   GDGTs in the analyzed marine sediment are dominated by hexamethylated (branched

238   GDGT-1050, Fig. 3B1) while tetramethylated derivatives (branched GDGT-1022, Fig.

239   3C1) are found predominantly in Messel shale. Such a difference in methylation patterns

240   is also reflected in their degradation derivatives, especially the monoallylethers, in which

241   the trimethylated component derived from branched GDGT-1050 is more abundant in the

242   marine sediment but the dimethylated representing branched GDGT-1022 is remarkable

243   in the Messel shale extracts (Fig. 4). Interestingly, no trimethylated diol and diallylether

244   are detected in the marine sediment sample, which implies that the branched GDGT-1050

245   in this marine subsurface sediment only in antiparallel form.

246

247   5. Conclusion and future applications

248   The glycerol configurations of GDGTs in both biological and environmental

249   samples can be determined by the composition of their chemical degradation derivatives

250   yielded by the selective *sn*2 ether cleavage protocol. Results of chemical degradation

251   confirm our previous report of GDGT glycerol configurations based on the distribution of

252   natural degradation derivatives. Combining data of natural and chemical degradation

253   derivatives allows us to conclude: (1) GDGTs in marine sediments are predominantly

254 configured with parallel glycerols; (2) AOM-related archaeal communities may have

255 contributed the antiparallel GDGTs in the environmental samples we analyzed; (3)

256 crenarchaeol and its so-called 'regioisomer' are both parallel with sn3,3 ether bonded

257 tricyclic biphytanyl moieties. Natural degradation derivatives of branched GDGTs were

258 not discussed in our previous work, but their chemical degradation derivatives, identified

259 here, indicate antiparallel dominates over the parallel configuration.

260 Many previous studies of lipid distributions and their carbon isotopic

261 compositions have shown that mixed planktonic and benthic sources contribute GDGTs

262 in marine sediment (e.g. Liu et al., 2011; Pearson et al., 2016 and references cited

263 therein). However, to date, no technique has been reported as capable of differentiating

264 them. The glycerol configurations of GDGTs synthesized by a broader range of archaeal

265 species should be investigated to verify whether marine *Thaumarchaeota* synthesize the

266 parallel configuration predominantly. Potential proxies based on the relative abundance

267 of mbpm versus bpdiol and dbpd can then be developed to investigate the impact of

268 benthic contribution to the total sedimentary GDGT pool.

269 Compared to biphytanes released by conventionally applied general ether

270 cleavage, mbpm and dbpd obtained from the selective sn2 ether cleavage contain both

271 glycerol and isoprenoid carbons. Their carbon isotopic compositions can reflect more

272 precisely the original signal of precursor GDGTs. If antiparallel GDGTs in marine

273 sediment are solely contributed by benthic archaea rather than synthesized by

274 *Thaumarchaeota*, then the carbon isotope composition of mbpm-0 should be distinct

275 from that of bpdiols and dbpds. Thus, the application of selective sn2 ether cleavage to

276 marine sedimentary GDGTs, followed by compound specific isotope analysis on mbpm,

277 bpdiol and dbpd can be an approach to potentially disentangle the mixed surface water

278 and sedimentary signals.

279

280 Acknowledgements

287

288

289

290

291 **References**

292 Bauersachs, T., Schouten, S., Schwark, L., 2014. Characterization of the sedimentary
293   organic matter preserved in Messel oil shale by bulk geochemistry and stable
294   isotopes. Palaeogeography, Palaeoclimatology, Palaeoecology 410, 390–400.

295 Dykstra, H.B., Lewis, J.F., Boord, C.E., 1930. A nuclear synthesis of unsaturated
296   hydrocarbons. I. alpha-olefins. Journal of the American Chemical Society 52, 3396–
297   3404.

298 Hayes, J.M., Takigiku, R., Ocampo, R., Callot, H.J., Albrecht, P., 1987. Isotopic
299   compositions and probable origins of organic-molecules in the Eocene Messel oil
300   shale. Nature 329, 48–51.

301 Gräther, O., Arigoni, D., 1995. Detection of regioisomeric macrocyclic tetraethers in the
302   lipids of Methanobacterium thermoautotrophicum and other archaeal organisms.
303   Journal of the Chemical Society, Chemical Communications 23, 405–406.

304 Liu, X.-L., Lipp, J.S., Hinrichs, K.-U., 2011. Distribution of core and intact GDGTs in
305   marine sediments. Organic Geochemistry 42, 368–375.

306 Liu, X.-L., De Santiago Torio, A., Bosak, T., Summons, R.E., 2016. Novel archaeal
307   tetraether lipids with a cyclohexyl ring identified in Fayetteville Green Lake, NY,
308   and other sulfidic lacustrine settings. Rapid Communications in Mass Spectrometry
309   30, 1197–1205.

310 Liu, X.-L., Lipp, J.S., Birgel, D., Summons, R.E., Hinrichs, K.U., 2018. Predominance of
311   parallel glycerol arrangement in archaeal tetraethers from marine sediments:
312   structural features revealed from degradation products. Organic Geochemistry 115,
313   12–23.

314 Pearson, A., Hurley, S.J., Walter, S.R.S., Kusch, S., Lichtin, S., Zhang, Y.G., 2016.
315   Stable carbon isotope ratios of intact GDGTs indicate heterogeneous sources to
316   marine sediments. Geochimica et Cosmochimica Acta 181, 18–35.

317 Sinninghe Damsté, J.S., Rijpstra, W.I.C., Hopmans, E.C., den Uijl, M.J., Weijers, J.W.H.,
318   Schouten, S., 2018. The enigmatic structure of the crenarchaeol isomer. Organic
319   Geochemistry 124, 22–28.

320 Sturt, H. F., Summons, R. E., Smith, K., Elvert, M., Hinrichs, K.-U., 2004. Intact polar
321   membrane lipids in prokaryotes and sediments deciphered by high-performance
322   liquid chromatography/electrospray ionization multistage mass spectrometry—new
323   biomarkers for biogeochemistry and microbial ecology. Rapid Communications in
324   Mass Spectrometry 18, 617–628.

325 Zhu, C., Lipp, J.S., Wörmer, L., Becker, K.W., Schröder, J., Hinrichs, K.-U., 2013.
326   Comprehensive glycerol ether lipids fingerprints through a novel reversed phase
327   liquid chromatography–mass spectrometry protocol. Organic Geochemistry 65, 53–
328   62.

Figure captions

330 **Fig. 1.** Hexose-phosphohexose-GDGT-0 as an example of intact polar archaeal

331 tetraethers showing the three general molecular components, namely, polar headgroups,

332 alkyl units and glycerol backbones, and structure variation resulted from the modification

333 of each component. Emphasized here are two types of glycerol configurations, the

334 parallel and antiparallel configurations.

335

336 **Fig. 2.** This chemical degradation scheme illustrates the distinct reaction products

337 generated by selective *sn*2 ether cleavage on GDGT-0 with different glycerol

338 configurations. Parallel GDGT-0 yields acyclic biphytanediol (bpdiol-0) and diallyl

339 biphytanyl diether (dbpd-0). Antiparallel GDGT-0, however, is degraded into two acyclic

340 monoallyl biphytanol monoethers (mbpm-0).

341

342 **Fig. 3.** Combined extracted ion chromatograms of LC–MS showing the composition of

343 GDGT core lipids in acid hydrolyzed intact polar lipids of *T. acidophilum* (A1) and TLEs

344 of marine sediment ODP201-1227A (B1) and Messel shale (C1), and the degradation

345 derivatives released via selective *sn*2 ether cleavage from *T. acidophilum* (A2), ODP201-

346 1227A (B2) and Messel shale (C2).

347

348 **Fig. 4.** LC–MS extracted ion chromatograms combined to illustrate the composition of

349 degradation derivatives of branched GDGTs in Messel shale (A) and ODP201-1227A (B).
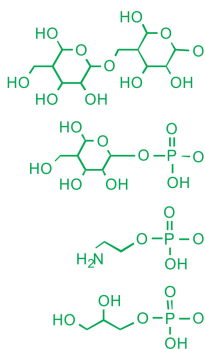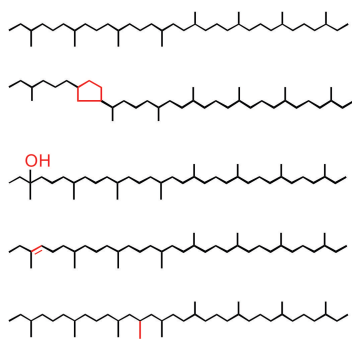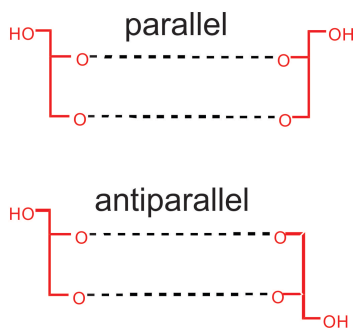
350

Hexose-phosphohexose-GDGT-0
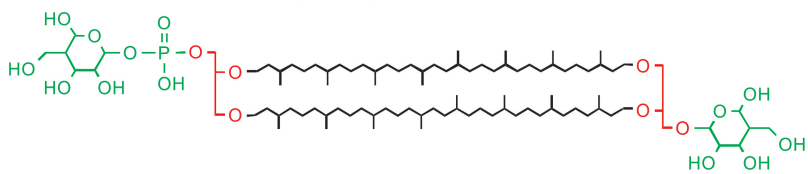
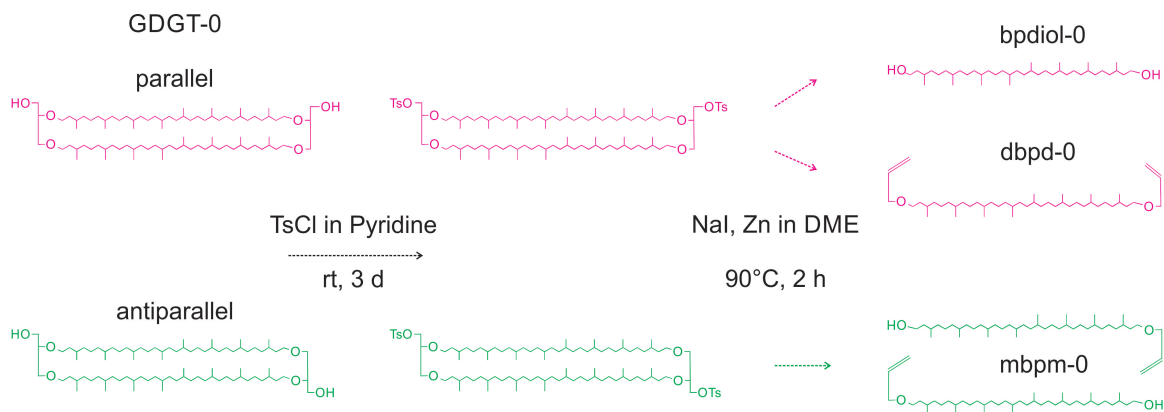| Polar headgroups	Alkyl units	Glycerol configurations

351

352

353

GDGT-0

parallel

bpdiol-0

dbpd-0

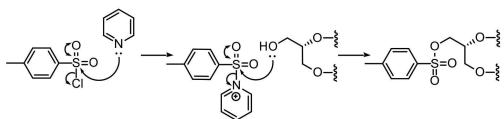TsCl in Pyridine
rt, 3 d

NaI, Zn in DME
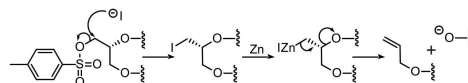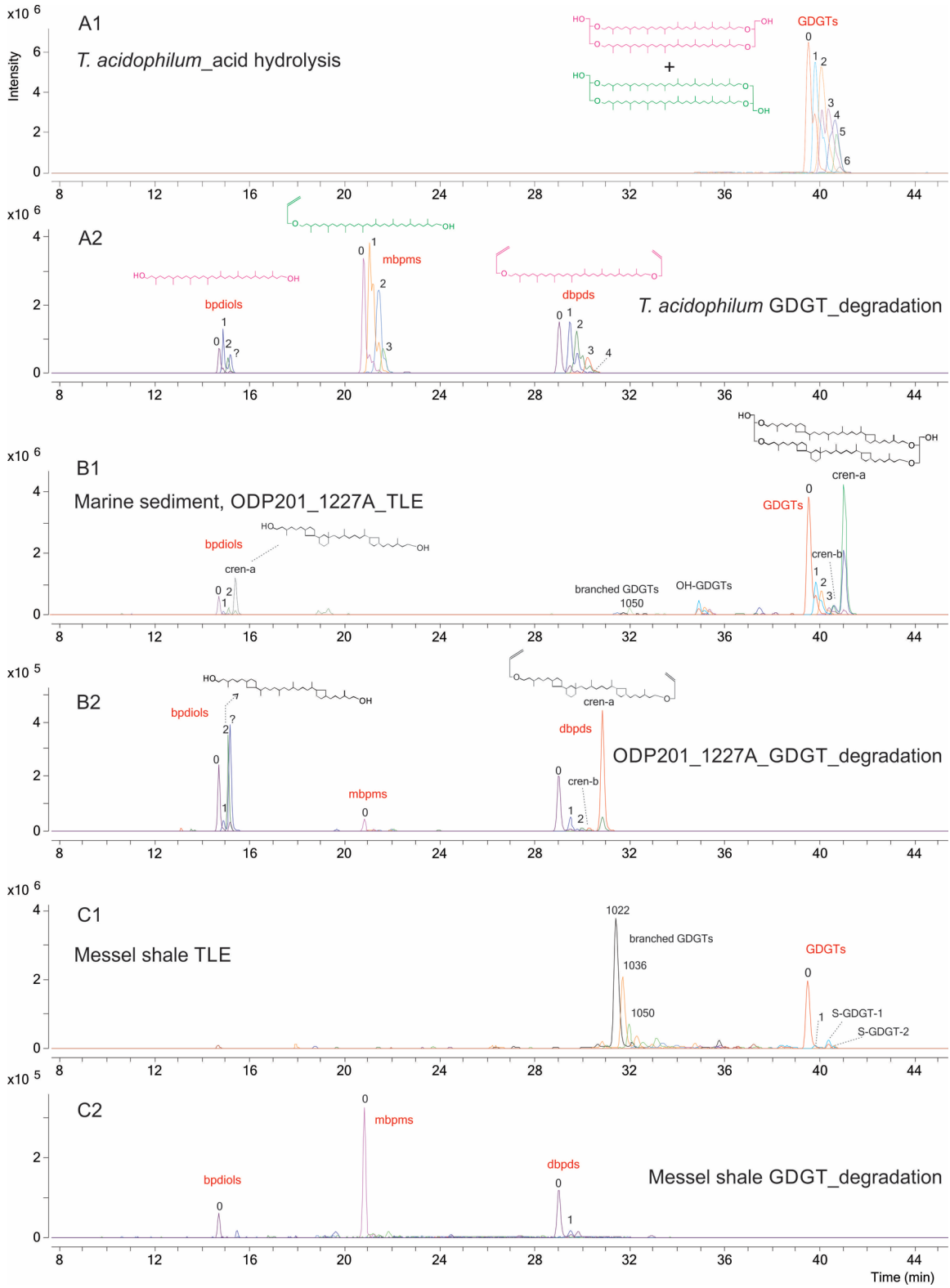90°C, 2 h

antiparallel

mbpm-0

Reaction (1)
Tosylation

Reaction (2)
Boord Haloalkoxy Elimination

354

355

359

360

361

362